Heliyon 10 (2024) e30434

Contents lists available at ScienceDirect

Heliyon

journal homepage: www.cell.com/heliyon

Research article

NMR-based metabolomic analysis of plasma from elderly patients with CVD before and after using contrast media

Qian Du [a,1], Ting Jiang [b,1], Qiuju Yuan [c], Yuanyuan Bai [c], Donghai Lin [b,**], Donghui Liu [c,d,*]

[a] Department of Cardiology, Guangzhou Red Cross Hospital, Medical College, Jinan University, Guangzhou, 510240, China
[b] Key Laboratory for Chemical Biology of Fujian Province, MOE Key Laboratory of Spectrochemical Analysis & Instrumentation, College of Chemistry and Chemical Engineering, Xiamen University, Xiamen 361005, China
[c] Department of Geriatrics, Guangzhou First People's Hospital, School of Medicine, South China University of Technology, Guangzhou, 510180, China
[d] Provincial Clinical Medicine College of Fujian Medical University, Department of Cardiology, Fujian Provincial Hospital, Fujian Cardiovascular Institute, Fujian Provincial Key Laboratory of Cardiovascular Disease, Fujian Provincial Center for Geriatrics, Fuzhou, 350001, China

ARTICLE INFO

Keywords:
NMR metabolomics
CVD
Contrast media
Plasma
Biomarkers

ABSTRACT

Contrast-induced acute kidney injury (CI-AKI) is a growingly common kidney problem caused by medical procedures involving contrast media (CM), especially in older patients with existing health issues. It is crucial to pinpoint potential biomarkers for the early detection of CI-AKI. Previously, we observed that iodixanol affects glucose, choline, and glutathione metabolism in endothelial cells under laboratory conditions. In this study, we used ^{1}H NMR-based metabolomics to examine the metabolic changes in the blood plasma of elderly patients with cardiovascular disease (CVD) before and after receiving iodixanol. We identified altered metabolites in plasma 24 and 48 h after iodixanol injection compared to levels before injection. Notably, metabolites such as glucose, unsaturated fatty acids (UFA), low-density lipoprotein (LDL)/very low-density lipoprotein (VLDL), pyruvate, choline, and glycine showed potential as biomarkers at 24 h post-injection compared to levels before injection. Similarly, glucose, pyruvate, lactate, choline, and glycine in plasma could serve as potential biomarkers at 48 h post-injection. Iodixanol notably affected pathways related to glycolysis, fatty acid breakdown, and amino acid metabolism according to our metabolic pathway analysis. The altered levels of specific metabolites in plasma could be indicative of CM-induced kidney injury. Overall, this research aids in understanding the physiological mechanisms involved and in identifying early biomarkers and prevention strategies for CI-AKI.

1. Introduction

Iodinated contrast media (CM) is widely utilized in diagnostic and therapeutic procedures for various ailments, including coronary

* Corresponding author. Department of Geriatrics, Guangzhou First People's Hospital, School of Medicine, South China University of Technology, Guangzhou, 510180, China.
** Corresponding author.
E-mail addresses: duqian1213@126.com (Q. Du), dhlin@xmu.edu.cn (D. Lin), eyliudh@scut.edu.cn (D. Liu).
[1] Q. D., and T. J. contributed equally to this work.

https://doi.org/10.1016/j.heliyon.2024.e30434
Received 20 February 2024; Received in revised form 24 March 2024; Accepted 25 April 2024
Available online 29 April 2024

Abbreviations

ACC	acetyl-CoA carboxylase
ACEI	angiotensin-converting enzyme inhibitor
ACS	acute coronary syndrome
AKI	acute kidney injury
ALT	alanine aminotransferase
AMPK	AMP-activated protein kinase
apoA-I	apolipoprotein A-I
ARB	angiotensin receptor blocker
AST	aspartate aminotransferase
CAG	coronary angiography
CCS	chronic coronary syndrome
CKD	chronic kidney disease
CM	contrast media
CI-AKI	contrast-induced acute kidney injury
CVD	cardiovascular disease
Cys-C	cystatin C
HDL-C	high-density lipoprotein cholesterol
KIM-1	kidney injury molecule-1
LDL	low-density lipoprotein
L-FABP	liver fatty acid-binding protein
NAc	N-acetyl
NAG	N-acetyl-beta-D-glucosaminidase
NGAL	neutrophil gelatinase associated lipid transporter protein
NMR	nuclear magnetic resonance
PBMCs	peripheral blood mononuclear cells
ROS	reactive oxygen species
SAP	stable angina pectoris
TCA	tricarboxylic acid
UFA	unsaturated fatty acid
VLDL	very low-density lipoprotein

angiography (CAG) and percutaneous coronary intervention (PCI) in patients with cardiovascular disease (CVD) [1,2]. Notably, CM is administered intravenously during these processes, potentially leading to systemic and organ-specific adverse reactions. Consequently, contrast-induced acute kidney injury (CI-AKI) occurs in up to 30 % of patients undergoing intravascular CM administration, ranking as the third most common cause of hospital-acquired AKI [3,4]. While most cases of CI-AKI are reversible, some patients experience persistent renal decline or even progress to end-stage renal disease without recovery of kidney function [5,6]. The precise pathophysiological mechanisms underlying CI-AKI remain incompletely understood, including renal vasoconstriction, renal medullary hypoxia, direct tubular toxicity, endothelial dysfunction, oxidative stress, apoptosis, and inflammation [6,7]. Currently, there are no effective treatments for CI-AKI, and accurate risk prediction is crucial for its prevention. However, predicting the risk of CI-AKI for individuals is challenging, despite assessing their medical histories (diabetes mellitus, hypertension, heart failure, chronic kidney disease, etc.) [4,8].

CI-AKI is identified by a sudden decline in glomerular filtration rate (GFR), followed by a rise in plasma creatinine levels or reduced urine output after intravascular injection of CM [9]. Consequently, elevated plasma creatinine is commonly used as a biomarker for diagnosing CI-AKI [10]. However, using plasma creatinine as a diagnostic marker has certain limitations. It increases gradually with declining GFR and only significantly changes in the later stages of CI-AKI [11]. This leads to delays and insensitivity in detecting renal injury, particularly when renal function is within normal ranges. Moreover, the increase in plasma creatinine only reflects glomerular damage rather than overall kidney injury and cannot serve as a real-time marker for changes in renal function [12]. Hence, there is an urgent need to discover novel biomarkers capable of indicating renal injury in the early stages of CI-AKI. In recent years, several emerging biomarkers have been identified as sensitive and early indicators of CI-AKI, including cystatin C (Cys-C), liver fatty acid-binding protein (L-FABP), neutrophil gelatinase-associated lipocalin (NGAL), N-acetyl-beta-D-glucosaminidase (NAG), and kidney injury molecule-1 (KIM-1) [13,14]. Additionally, the potential of circulating microRNA and small molecule metabolites has also garnered significant attention [15].

Metabolomics has emerged as a potent tool for identifying disease-related biomarkers and elucidating the connections between metabolites [16]. This analytical approach enables quantitative assessment of metabolite levels in biological samples [17,18], offering a novel means of predicting the risk of various diseases, including renal injury [19]. In studies involving CI-AKI rats, researchers identified 30 metabolites in the kidney, plasma, and urine associated with renal injury, spanning 9 metabolic pathways including energy metabolism, amino acid metabolism, and inflammatory responses [20]. Urine metabolomics research revealed that higher

levels of citrate and taurine prior to CM injection correlated with reduced incidence of renal damage, while concentrations of urine xylose, glycine, uric acid, and threonic acid significantly increased post-CM use [21]. NMR-based metabolomic analysis indicated that changes in urinary metabolites strongly correlated with renal damage in patients administered low osmolar iopromide, potentially serving as biomarkers for predicting CI-AKI risk [22]. In a cohort study, metabolomic analysis demonstrated a positive correlation between urine metabolite concentrations and the severity of renal injury induced by iodixanol, offering a multi-metabolite model for early CI-AKI prediction [23].

Previously, our research revealed that iodixanol activated glucose metabolism and the tricarboxylic acid (TCA) cycle while inhibiting choline and glutathione metabolism, leading to oxidative stress, apoptosis, and inflammation in endothelial cells [24,25]. However, monitoring plasma metabolomic changes in patients undergoing CM injection is crucial for early CI-AKI detection. In this study, we investigated plasma metabolic alterations in patients with CVD before CM injection, and at 24 and 48 h post-procedure using NMR-based metabolomic analyses. Our findings demonstrate significant changes in plasma metabolic profiles following CM injection, potentially offering a panel of biomarkers for early CI-AKI prediction based on these characteristic metabolites.

2. Materials and methods

2.1. Study subjects and ethics statement

Thirty-eight patients with CVD were recruited from Fujian Provincial Hospital (Fuzhou, China) and underwent cardiac catheterization and percutaneous coronary intervention (PCI) therapy between April 15 and October 31, 2020. The inclusion criteria were as follows: (1) Subjects diagnosed with chronic coronary syndrome (CCS) and stable angina pectoris (SAP) according to established diagnostic criteria [26], (2) aged between 60 and 80 years, (3) provided informed consent, and (4) underwent coronary angiography (CAG) and PCI procedures involving approximately 100–120 ml intravenous injection of iodixanol (Visipaque, 320 mg I/ml, GE Healthcare, Chicago, IL, USA). The exclusion criteria comprised four criteria, and patients failing to meet any of these criteria were excluded. The criteria were: (1) Acute coronary syndrome (ACS), acute heart failure, and acute cerebrovascular disease; (2) Chronic kidney disease (CKD) stage 3–5, and severe liver dysfunction; (3) Patients with psychosis or inability to understand the informed consent properly; and (4) Patients with acute infectious diseases and cancer.

This study was conducted following the principles outlined in the Declaration of Helsinki. Ethical approval was obtained from the Ethics Committee of Fujian Provincial Hospital (No. K2020-03-077, approval date: March 30, 2020). All participants provided written informed consent for their involvement in this study, including diagnostic evaluations and interventional procedures.

2.2. Plasma sample collection and NMR sample preparation

Approximately 5 ml of venous blood was collected from each subject after an 8-h fast, into a heparin tube, before iodixanol injection, and at 24 and 48 h post-procedure, and immediately placed at 4 °C. Within half an hour, plasma was separated by centrifugation at 3000 rpm at 4 °C for 15 min. The upper plasma layer was collected and stored at −80 °C. For NMR analyses, frozen plasma samples were thawed at 4 °C, and then 350 μl of plasma was mixed with 100 μl of D_2O (99.99 %, Sigma, USA) and 100 μl of phosphate buffer (0.1 M, pH 7.4), vortexed for 3 min, and centrifuged at 12,000 rpm at 4 °C for 15 min. Subsequently, 500 μl of supernatant was transferred into a 5-mm NMR tube for analysis [27].

2.3. ^1H NMR spectrum measurements

^{1}H NMR analyses were conducted at 298 K using a Bruker AVANCE III HD 850 MHz spectrometer (Bruker BioSpin, Germany) equipped with a TCI cryoprobe at 25 °C. One-dimensional (1D) ^{1}H NMR spectra were acquired employing the Carr–Purcell–Meiboom–Gill (CPMG) pulse sequence [RD-90°-(τ-180°-τ)n-ACQ] with water suppression. RD represented the relaxation delay (4 s) and τ denoted the spin echo delay (300 μs). A total of 64 transients were accumulated into 64 K data points with a spectrum width (SW) of 20 ppm and an acquisition time (ACQ) of 2.73 s.

2.4. NMR data processing

NMR spectra were imported into MestReNova software (version 9.0, Mestrelab Research S.L, Spain) for data processing. Both phasing and baseline correction were performed manually. Chemical shift calibration was referenced to the methyl group of TSP at 0.0 ppm. Spectral regions corresponding to water resonance (δ 4.7−5.1) were excluded. Spectral regions spanning δ 0.5−8.6 were segmented into bins with a width of 0.002 ppm. Subsequently, metabolite integrals were extracted from each 1D ^{1}H NMR spectrum using MATLAB (Version Matlab2015b; MathWorks, USA), and normalized by the integral of TSP in each spectrum. The relative level of each metabolite was calculated based on the relative integrals of singlet or non-overlapping peaks of the metabolite. The number of protons contained in the corresponding hydrogen-containing group of the metabolite was represented as mean ± standard deviation (SD) for each group of plasma samples.

2.5. Multivariate statistical analyses and identification of differential metabolites

Multivariate statistical analysis was performed using SIMCA-P software (Version 14.1, Umetrics AB, Umeå, Sweden). The pareto

scaling method was applied to the normalized spectral integrals to amplify the magnitude of low-level metabolites without significantly amplifying noise. An unsupervised principal component analysis (PCA) was conducted to visualize metabolic profile trends, identify outliers, and delineate metabolic clusters among the samples. Additionally, a supervised orthogonal projection on latent structure with discriminant analysis (OPLS-DA) was executed to enhance metabolic classifications and pinpoint variables significantly contributing to metabolic distinctions. Data filtering was employed to remove variables not commonly used in modeling, such as baselines and noise, using the interquartile range (IQR) method. Prior to multivariate statistical analysis, data preprocessing involved automatic scaling, centering on the mean and dividing by the standard deviation of each variable. This scaling approach maintained data integrity while reducing the weight of larger variables (high-level metabolites) and increasing the weight of smaller variables (low-level metabolites). The reliability of established OPLS-DA models was assessed using response permutation tests with 200 cycles.

Load plots with color (red, yellow, and blue) were constructed to identify variables that changed significantly, very significantly, and insignificantly, respectively. Important metabolites were identified based on the absolute value of correlation coefficient ($|r| \geq$ absolute value) and variable importance in projection (VIP $\geq$1). The reliability of the OPLS-DA model was further verified through cross-validation plots derived from permutation tests (n = 200), where two model parameters, R^2Y and Q^2, were indicative of model reliability. R^2Y represented the goodness of fit of the model, while Q^2 reflected model accuracy. Values closer to 1 for these parameters indicated better stability and robustness of the OPLS-DA model.

R^2 and Q^2 serve as indicators of the reliability of OPLS-DA models, with R^2 representing the model's explanatory power and Q^2 representing its predictive accuracy. Higher values closer to 1 indicate greater reliability of the OPLS-DA model. VIP scores for metabolites were computed using SIMCA-P software. The OPLS-DA models were utilized to pinpoint significant metabolites primarily responsible for the observed metabolic differences among the three groups. Significant metabolites were identified based on two criteria: VIP scores $\geq$1 and correlation coefficients $|r| \geq$ the critical value corresponding to statistical significance ($p < 0.05$).

2.6. Metabolic pathway analysis

Metabolic pathway analysis was conducted to identify significantly perturbed metabolic pathways based on the relative concentrations of assigned metabolites. This analysis utilized the Pathway Analysis module provided by MetaboAnalyst 5.0 (https://www.metaboanalyst.ca). The following parameters were selected: Enrichment method (Hypergeometric test), Topology analysis (Relative-betweeness centrality), Pathway library (Homo sapiens, KEGG). Metabolic pathways with -lg(p) scores >3 and pathway impact values (PIVs) > 0.2 were considered significantly altered.

2.7. Identification of potential biomarkers based on the disturbed metabolic pathways

Metabolomic analysis is commonly employed to identify potential biomarkers for early disease diagnosis [28]. In this study, 2/3 of the plasma samples were randomly selected for receiver operating characteristic (ROC) curve analysis to assess the contribution of metabolites involved in the perturbed metabolic pathways. In the multivariate ROC curve analysis, logistic regression algorithm was employed for classification, and the area under curve (AUC) value was used to evaluate the predictive performance of selected biomarkers. Initially, multivariate ROC curve analysis was performed on all characteristic metabolites identified between groups,

Table 1
Clinical characteristics of subjects.

Clinical characteristics	Patients (n = 38)
Baseline findings	
Age (years)	69.74 ± 9.75
Gender (male/female)	28/10
Smoking	15
Hypertension	29
Diabetes	15
Laboratory findings	
Hemoglobin (g/L)	132.43 ± 18.39
Albumin (g/L)	40.54 ± 4.51
Total cholesterol (mmol/L)	3.75 ± 1.44
HDL-C (mmol/L)	1.10 ± 0.49
LDL-C (mmol/L)	2.39 ± 1.11
Creatinine (μmol/L)	109.74 ± 40.36
BUN (mmol/L)	7.63 ± 2.33
ALT (μ/L)	23.69 ± 14.35
AST (μ/L)	27.38 ± 15.90
Medications	
Aspirin	32
Clopidogrel	38
Indobufen	6
ACEI/ARB	25
β-blocker	30
Statins	38
Diuretics	3

calculating AUC values for each metabolite and all metabolites combined. Subsequently, multivariate ROC curve analysis was repeated for characteristic metabolites with AUC values > 0.70. Finally, single metabolites or combinations of metabolites with AUC values > 0.70 were identified as potential biomarkers for early detection of renal injury. Confirmation of potential biomarkers' validity was conducted using multivariate ROC analysis with the remaining 1/3 of the plasma samples.

2.8. Student's t-test

We computed spectral integrals based on characteristic NMR peaks. Independent sample t-tests were conducted to validate the differential metabolites using SPSS software (Version 22.0, Chicago, IL, USA). The average metabolite integrals were presented as Mean ± SD. Variables with p-values <0.05 were considered statistically significant ($^{*}p < 0.05$, $^{**}p < 0.01$, $^{***}p < 0.001$). In addition, we also performed Tukey' s Honestly Significant Difference to control the false discovery rate for multiple comparisons (Supplement).

3. Results

3.1. Characterization of subjects

A total of 38 inpatients, comprising 28 males and 10 females, were included in this study. All subjects met the criteria for CCS and SAP and received intravenous injections of iodixanol along with PCI treatment during hospitalization. As shown in Table 1, the average age was 69.74 ± 9.75 years, with all subjects being over 60 years old. All 38 patients were engaged in venous blood collection at 0 h (prior to iodixanol administration) and 24 h (post iodixanol injection), and 22 patients were collected venous blood at 48 h (post iodixanol injection).

3.2. Metabolite recognition and changed metabolic profiles of plasma

All metabolites were identified using Chenomx NMR Suite software and the HMDB database, resulting in a total of 27 identified metabolites (Fig. 1). The NMR resonance signals of these metabolites are presented in Table 2, including lactate, leucine, 3-hydroxybutyrate, ethanol, alanine, acetate, isoleucine, N-acetyl (NAc), low-density lipoprotein (LDL)/very low-density lipoprotein (VLDL), citrate, valine, glutamine, threonine, creatinine, pyruvate, lysine, malonate, choline, glycine, glucose, urea, unsaturated fatty acid (UFA), lipids, tyrosine, histidine, formate, and phenylalanine.

To investigate the impact of iodixanol on plasma metabolic patterns, pairwise supervised partial least squares-discriminant analysis (PLS-DA) models were constructed. PLS-DA three-dimensional score plots revealed a distinct difference in metabolic profiles between 24 and 48 h after iodixanol injection compared to baseline (0 h), with more overlapping samples between 24 and 48 h post-injection (Fig. 2A). Subsequently, supervised orthogonal partial least squares-discriminant analysis (OPLS-DA) analysis was performed to identify important metabolites between these groups. The metabolic signature of plasma at 24 and 48 h post-iodixanol injection was well distinguished from baseline (0 h) in the first principal component (t [1]) (Fig. 2B). The reliability and robustness of the two OPLS-DA models were confirmed by R^2Y and Q^2 values, along with corresponding model cross-validation diagrams (Fig. 2C). Notably, there was significant overlap between the sample points at 24 and 48 h post-injection in t [1], indicating a lack of clear distinction between these two groups (Fig. 2C). Thus, iodixanol exerted a significant effect on the metabolic profile of plasma in elderly patients with CVD.

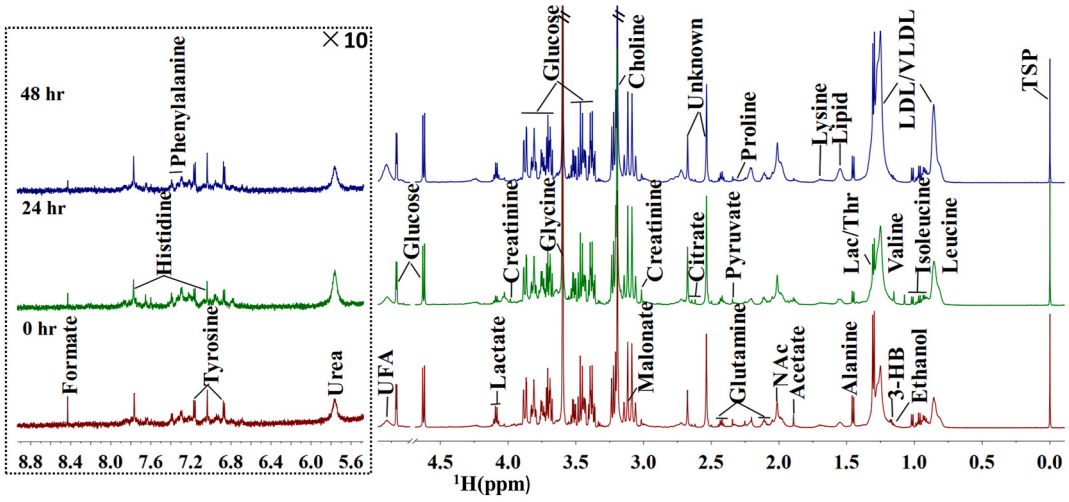

Fig. 1. The typical 1D ^{1}H NMR spectra of plasma from elderly patients with CVD before and after injecting iodixanol. From bottom to top: 0 h (prior to iodixanol administration), 24 h, and 48 h (post iodixanol injection).

Table 2
Chemical shifts of metabolites from 1D ^{1}H NMR spectra in plasma.

NO.	Metabolites	δ 1H (ppm) and multiplicy	Moieties#
1	Leucine	0.96(d),0.97(d),1.69(m),1.70(m),1.73(m), 3.73(m)	α-CH_3, α-CH_3, γ-CH, β-CH_2, α-CH
2	Isoleucine	0.94(t),1.01(d),1.21(m),1.42(m),2.00(m), 3.67(d)	δ-CH_3, γ-CH_3, half γ-CH_2, half γ-CH_2, β-CH, α-CH
3	Valine	0.99(d), 1.05(d), 2.26(m), 3.60(d)	γ-CH_3, γ-CH_3, β-CH, α-CH
4	LDL/VLDL	0.89(bar),1.28(bar)	
5	3-HB[a]	1.197(d),2.314(m),2,394(m), 4.142(m)	γ-CH_3,β-CH_2,γ-CH,
6	Lipid	0.82–0.90(bar),1.24–1.31(bar)	
7	Ethanol	1.17 (t), 3.65 (q)	δ-CH_3, CH_2
8	Lactate	1.33(d), 4.11(q)	β-CH_3, α-CH
9	Threonine	1.30(d), 3.58(d), 4.24(m)	γ-CH_2, β-CH
10	Alanine	1.47(d), 3.78(q)	β-CH_3, α-CH
11	Lysine	1.43(m),1.49(m),1.70(m), 1.91(m),3.02(t),3.75(t)	halfγ-CH_2, halfγ-CH_2, δ-CH_2,β-CH_2, ε-CH_2, α-CH
12	Acetate	1.91(s)	CH_3
13	NAc[a]	2.02–2.06(bar)	CH_3
14	Citrate	2.51(d),2.68(d)	β-CH_2
15	Glutamine	2.13(m), 2.45(m), 3.77(t)	γ-CH_2, β-CH_2, α-CH
16	Pyruvate	2.38(s)	α-CH_3
17	Malonate	3.13(s)	CH_2
18	Creatinine	3.03(s),4.05(s)	N–CH_3,CH_2
19	Choline	3.21(s), 3.51(dd),4.04(t)	N-$(CH_3)_3$, α-CH_2,CH_2OH
20	Glycine	3.57(s)	α-CH_2
21	Glucose	β(3.24(dd), 3.48(t), 3.90(dd)), α(3.54(dd), 3.71(t), 3.72(dd), 3.83(m))	β(H_2, H_3, H_5), α(H_2, H_3, H_6)
22	Urea	5.78(bar)	NH_2
23	UFA[a]	5.23–5.38(bar)	
24	Tyrosine	3.05(dd),3.19(dd),6.92(d), 7.19(d)	halfβ-CH_2,halfβ-CH_2,β-CH, α-CH
25	Histidine	7.06(s),7.85(s)	^{5}CH,^{2}CH
26	Formate	8.46(s)	CH
27	Phe[a]	3.12(dd),3.30(dd),3.99(dd), 7.33(d),7.37(t),7.43(t)	α-CH,halfβ-CH_2,halfβ-CH_2, α-CH,β-CH,γ-CH

Note: #: s, single; d, double; t, triplet; q, quartet; m, multiple; dd, double of double.
[a] 3-HB, 3-hydroxybutyric acid; NAc, N-acetyl; UFA, unsaturated fatty acid; Phe, phenylalanine.

3.3. Identification of significant metabolites

Using VIP values and load weight correlation coefficients (Pcorr) from the OPLS-DA model, loading plots were established between groups. Metabolites on the loading plots were identified based on metabolite recognition from ^{1}H NMR spectral data. Results revealed 7 important metabolites: LDL/VLDL, NAc, glucose, UFA, creatinine, choline, and glycine between the 24-h (post-iodixanol injection) group and the 0-h (prior to iodixanol administration) group (Fig. 3A). In the 48-h group (post-iodixanol injection), 6 altered important metabolites relative to the 0-h group were identified, including LDL/VLDL, ethanol, glucose, lactate/threonine, choline, and glycine (Fig. 3B). Additionally, increased levels of LDL/VLDL and glucose, as well as decreased levels of choline and glycine in plasma, were observed at 48 h post-iodixanol injection compared to those at 24 h post-injection.

3.4. Identification and quantitative analysis of differential metabolites

To assess the changes in plasma metabolites induced by iodixanol injection, absolute integral values of metabolites were calculated based on characteristic NMR peaks. At 24 h post-injection *vs.* baseline (0 h), a total of 8 differential metabolites ($p < 0.05$) were identified, including LDL/VLDL, lipids, NAc, glucose, UFA, pyruvate, choline, and glycine (Table 3). Similarly, at 48 h post-injection *vs.* baseline, 6 differential metabolites ($p < 0.05$) were identified, including ethanol, glucose, lactate, pyruvate, choline, and glycine.

Increased level of pyruvate was a differential metabolite instead of an important metabolite. By combining differential metabolites identified by the *t*-test with important metabolites identified by OPLS-DA analysis, changes in creatinine, lipid, pyruvate, and LDL/VLDL levels were examined. At 24 h post-injection, creatinine levels significantly increased as an important metabolite in OPLS-DA analysis, although there were no changes in the *t*-test analysis compared to the baseline group. Additionally, decreased lipid levels and increased pyruvate concentrations were identified as differential metabolites, despite no statistical changes in OPLS-DA analysis. At 48 h post-injection *vs.* baseline, decreased LDL/VLDL levels were identified as important metabolites instead of differential metabolites. Conversely, increased pyruvate levels were identified as differential metabolites rather than important metabolites.

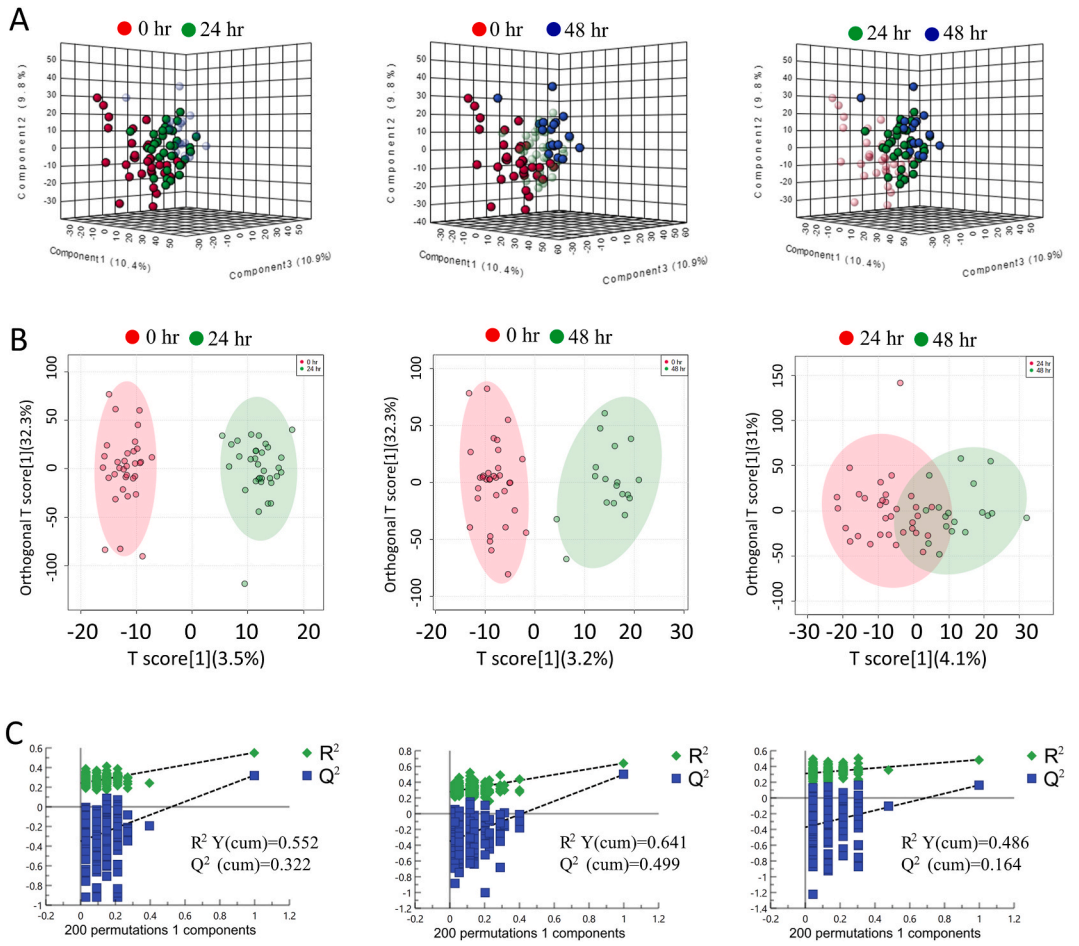

Fig. 2. PLS-DA 3D scores plots and OPLS-DA scores plots for 1D ^{1}H NMR spectra recorded from. (A) PLS-DA 3D scores plots at 0 h (prior to iodixanol administration), 24 h, and 48 h (post iodixanol injection); (B) OPLS-DA scores plots of pairwise groups; (C) Cross-validation plots from permutation tests of the OPLS-DA models (n = 200). From left to right: 24 h (post iodixanol injection) *vs.* 0 hr (prior to iodixanol administration), 48 h (post iodixanol injection) *vs.* 0 hr (prior to iodixanol administration), 48 h (post iodixanol injection) *vs.* 24 hr (post iodixanol injection).

3.5. Quantitative analysis of characteristic metabolites

Based on important and differential metabolites, characteristic metabolites among groups were identified, with each metabolite's contribution described by VIP values ranking. At 24 h post-iodixanol injection *vs.* baseline, 8 characteristic metabolites and their absolute integral value ranking were identified, including glucose, UFA, LDL/VLDL, NAc, lipids, pyruvate, choline, and glycine (Fig. 4A). Similarly, at 48 h post-iodixanol injection *vs.* baseline, 8 characteristic metabolites (glucose, ethanol, LDL/VLDL, UFA, choline, glycine, lactate, and pyruvate) were found to contribute to differences in metabolic patterns (Fig. 4B). Notably, 6 characteristic metabolites were shared at both 24 and 48 h post-iodixanol injection. Glycine, choline, and glucose exhibited potent contributions to distinguished metabolic profiles based on their larger VIP scores. To visually compare concentration changes of characteristic metabolites in plasma at 24 and 48 h, fold change values of metabolites were displayed on a histogram (Fig. 4C). Pyruvate, choline, glycine, and glucose were statistically changed at both time points. Levels of choline and glycine significantly increased ($p < 0.001$), while glucose significantly decreased ($p < 0.001$) at 24 h post-injection.

3.6. Significantly changed metabolic pathway analysis

The absolute integral values were submitted to the pathway analysis module on the MetaboAnalyst 5.0 website. Significantly altered metabolic pathways induced by iodixanol were identified based on criteria of $p < 0.05$ and PIV >0.2. In comparison to baseline (0 h, prior to iodixanol administration), three notable metabolic pathways were discerned at 24 h post-iodixanol injection (Fig. 5A): glycine, serine, and threonine metabolism (a), starch and sucrose metabolism (b), and pyruvate metabolism (c). Remarkably, these same pathways were consistently identified at 48 h post-iodixanol injection (Fig. 5B). Furthermore, a comprehensive diagram integrating metabolites was generated based on the HMDB and KEGG databases, illustrating the metabolic pathway of these compounds

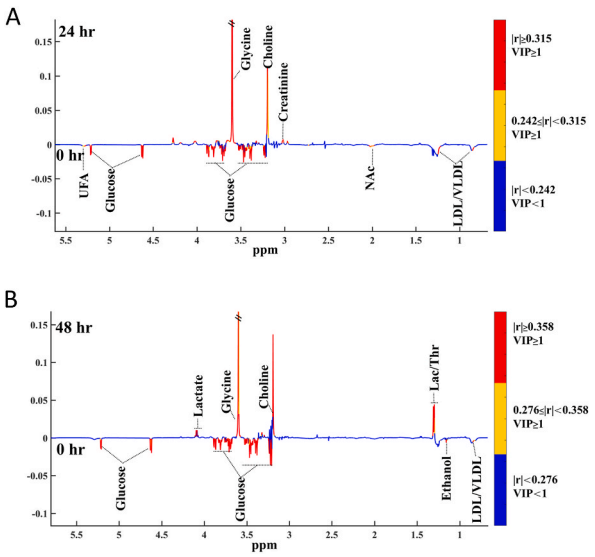

Fig. 3. Correlation coefficient-coded loading plots from OPLS-DA model. The color pattern of the loading plot was used to identify the significant metabolites in the class separation. Red, yellow, and blue denote that the variables were very significant, significant, and insignificant, respectively. (A) Loading plot in 24 h (post iodixanol injection) *vs.* 0 hr (prior to iodixanol administration); (B) Loading plot in 48 h (post iodixanol injection) *vs.* 0 hr (prior to iodixanol administration). (For interpretation of the references to color in this figure legend, the reader is referred to the Web version of this article.)

Table 3
Differential metabolites ($p < 0.05$) were identified from Student's *t* tests between 24 h (post iodixanol injection) *vs.* 0 hr (prior to iodixanol administration) and 48 h (post iodixanol injection) *vs.* 0 hr (prior to iodixanol administration).

Metabolite	Mean ± SD			Student's *t*-test	
	0 h (n = 38)	24 h (n = 38)	48 h (n = 22)	24 h *vs.* 0 hr	48 h *vs.* 0 hr
Glucose metabolism					
Glucose	1.49 ± 0.07	1.19 ± 0.05	1.19 ± 0.08	***	**
Pyruvate	0.12 ± 0.00	0.13 ± 0.00	0.13 ± 0.00	*	*
Lactate	0.71 ± 0.04	0.73 ± 0.02	0.95 ± 0.07	ns	**
Fatty acid metabolism					
UFA*	1.45 ± 0.07	1.15 ± 0.05	1.26 ± 0.08	**	ns
NAc*	1.53 ± 0.04	1.37 ± 0.04	1.48 ± 0.04	**	ns
Lipid	0.86 ± 0.06	0.71 ± 0.04	0.80 ± 0.07	*	ns
LDL/VLDL	5.74 ± 0.19	4.96 ± 0.17	5.27 ± 0.19	**	ns
Choline	8.74 ± 0.24	10.55 ± 0.30	10.41 ± 0.36	***	**
Amino acid metabolism					
Leucine	0.93 ± 0.02	0.87 ± 0.02	0.95 ± 0.02	ns	ns
Isoleucine	0.17 ± 0.01	0.17 ± 0.01	0.19 ± 0.01	ns	ns
Valine	0.35 ± 0.01	0.33 ± 0.01	0.36 ± 0.01	ns	ns
3-HB*	0.41 ± 0.01	0.41 ± 0.02	0.39 ± 0.01	ns	ns
Ethanol	0.52 ± 0.03	0.53 ± 0.05	0.42 ± 0.02	ns	*
Threonine	4.64 ± 0.21	4.16 ± 0.17	5.40 ± 0.34	ns	ns
Alanine	0.62 ± 0.02	0.65 ± 0.03	0.66 ± 0.03	ns	ns
Lysine	0.66 ± 0.02	0.65 ± 0.02	0.70 ± 0.02	ns	ns
Acetate	0.10 ± 0.00	0.11 ± 0.01	0.09 ± 0.00	ns	ns
Citrate	0.25 ± 0.01	0.25 ± 0.01	0.25 ± 0.01	ns	ns
Glutamine	0.50 ± 0.02	0.53 ± 0.02	0.53 ± 0.02	ns	ns
Malonate	2.43 ± 0.06	2.42 ± 0.06	2.44 ± 0.08	ns	ns
Creatinine	0.30 ± 0.01	0.46 ± 0.08	0.33 ± 0.02	ns	ns
Glycine	10.06 ± 0.38	14.41 ± 0.61	13.40 ± 0.58	***	***
Urea	0.27 ± 0.02	0.25 ± 0.01	0.25 ± 0.01	ns	ns
Tyrosine	0.08 ± 0.00	0.08 ± 0.00	0.09 ± 0.00	ns	ns
Histidine	0.07 ± 0.00	0.07 ± 0.00	0.07 ± 0.00	ns	ns
Formate	0.02 ± 0.00	0.02 ± 0.00	0.02 ± 0.00	ns	ns
Phe*	0.21 ± 0.01	0.21 ± 0.01	0.23 ± 0.01	ns	ns

Note: ***, **, * denote $p < 0.001$, $p < 0.01$, $p < 0.05$, respectively; red/blue indicate increased/decreased levels of metabolites.

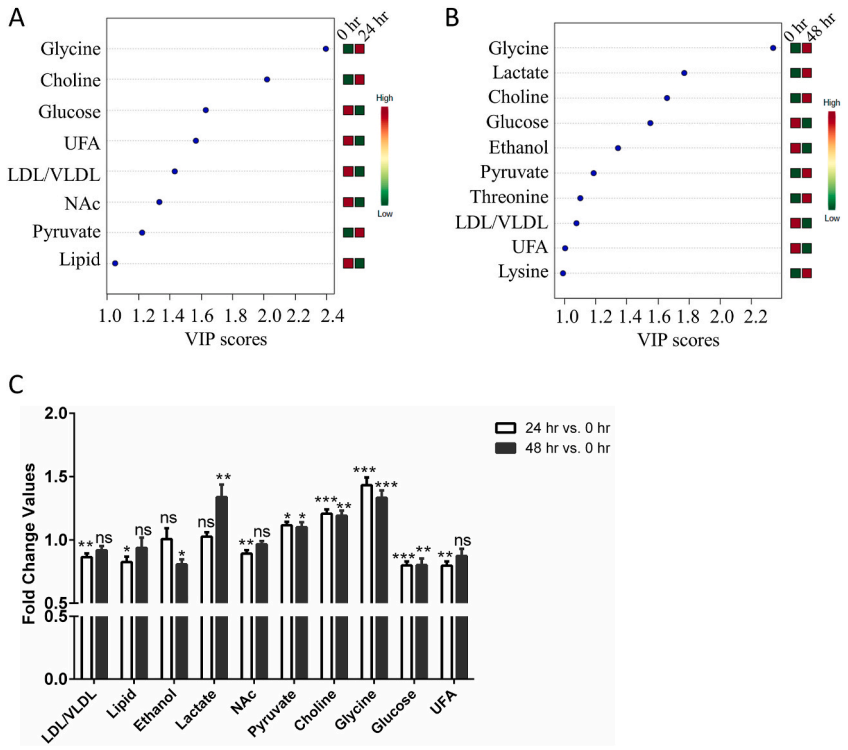

Fig. 4. VIP ranking of characteristic metabolites from pairwise group. (A) VIP ranking plots of characteristic metabolites at 24 h (post iodixanol injection) *vs.* 0 hr (prior to iodixanol administration); (B) VIP ranking plots of characteristic metabolites at 48 h (post iodixanol injection) *vs.* 0 hr (prior to iodixanol administration); (C) Fold change values of characteristic metabolites between 24 h (post iodixanol injection) *vs.* 0 hr (prior to iodixanol administration) and 48 h (post iodixanol injection) *vs.* 0 hr (prior to iodixanol administration). In addition, we also performed Tukey' s Honestly Significant Difference to control the false discovery rate for multiple comparisons.

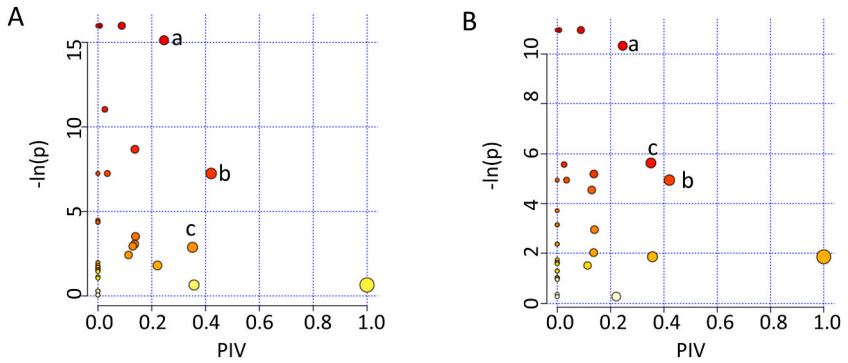

Fig. 5. Significantly altered metabolic pathways at 24 h and 48 h (post iodixanol injection). (A) Pathway bubble chart at 24 h (post iodixanol injection) *vs.* 0 hr (prior to iodixanol administration); (B) Pathway bubble chart at 48 h (post iodixanol injection) *vs.* 0 hr (prior to iodixanol administration). a: glycine, serine, and threonine metabolism; b: starch and sucrose metabolism; c: pyruvate metabolism.

(Fig. 6). Notably, alterations in plasma metabolite levels before and after iodixanol injection predominantly pertained to glycolysis and glycine, serine, and threonine metabolic pathways.

3.7. Potential biomarkers in plasma

To assess the significance and predictive capability of characteristic metabolites for CM-induced kidney injury, we conducted multivariate ROC curve analysis. Notably, the AUC values of characteristic metabolites exceeded 0.50, with nearly half surpassing 0.70 at both 24 and 48 h post-iodixanol injection compared to baseline (0 h group) (Fig. 7A and C), indicating their strong predictive potential. Specifically, at 24 h post-injection, the AUC values of characteristic metabolites (glucose, LDL/VLDL, pyruvate, choline,

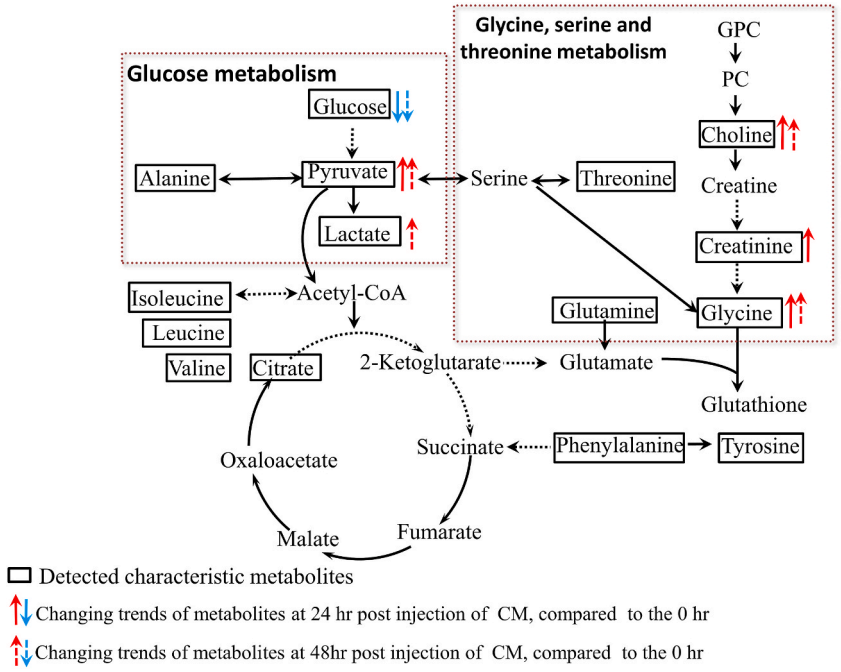

Fig. 6. Schematic diagram of metabolic pathways involved in metabolites.

glycine, and UFA) surpassed 0.70 (Fig. 7B), and at 48 h post-injection, metabolites (glucose, pyruvate, lactate, choline, and glycine) exhibited AUC values exceeding 0.70 (Fig. 7D). Furthermore, multivariate ROC analysis of characteristic metabolites with AUC >0.70 demonstrated superior predictive performance compared to single metabolites, with AUC values of 0.910 at 24 h and 0.905 at 48 h post-injection (Fig. 7B and D), underscoring the effectiveness of metabolite combinations for prediction.

Additionally, we evaluated the reliability of significantly altered metabolic pathways identified through metabolic pathway analysis using multivariate ROC curve analysis of all involved metabolites. Notably, significantly changed metabolic pathways at 24 h post-iodixanol injection consistently exhibited higher AUC values. Specifically, AUC values were 0.891 for glycine, serine, and threonine metabolism, 0.732 for starch sucrose metabolism, and 0.713 for pyruvate metabolism (Fig. 8 A, B, and C). Similarly, at 48 h post-injection, altered metabolic pathways displayed AUC values of 0.896 for glycine, serine, and threonine metabolism, 0.719 for starch, sucrose metabolism, and 0.823 for pyruvate metabolism (Fig. 8D, E, and F). These findings underscored the reliability and importance of the three significantly altered metabolic pathways. Furthermore, a positive correlation was observed between AUC value and p-value for each metabolic pathway, further validating their predictive potential.

4. Discussion

With the burgeoning employment of CM in the diagnostic and treatment processes of numerous diseases, CI-AKI emerged as a prevalent iatrogenic kidney ailment [4,6]. This potentially severe complication extended hospital stays, heightened cardiovascular incidents, escalated the risk of end-stage kidney disease, and elevated mortality rates, particularly among elderly patients with underlying conditions [29]. Typically, the surge in plasma creatinine levels following CM injection serves as the diagnostic hallmark of CI-AKI. Nonetheless, creatinine levels witness a significant elevation only towards the conclusion of renal injury, underscoring the necessity for early biomarkers to predict CI-AKI [11]. Herein, we conducted ^{1}H NMR-based metabolomics on plasma samples from elderly patients with CVD before and after iodixanol administration. By pinpointing metabolic alterations induced by CM, timely preventive measures can be implemented to mitigate the onset of clinical complications.

4.1. CM-activated glycolysis pathway

Relative to the baseline at 0 h (prior to iodixanol administration), there were significant alterations in glucose metabolism within metabolic pathways at both 24 and 48 h following iodixanol injection. We consistently observed decreased levels of glucose and increased levels of pyruvate at 24 and 48 h compared to the 0-h counterparts. Furthermore, glucose and pyruvate, identified as characteristic metabolites, exhibited large AUC values (0.732 and 0.719 for the 24-h group *vs.* 0-hour group; 0.724 and 0.717 for the 48-h group *vs.* 0-hour group), suggesting their potential as plasma biomarkers. Notably, in the comparison between the 48-h group and the 0-h group, plasma lactate levels showed a significant increase with a high AUC value (0.746), indicating the activation of glycolysis metabolism following iodixanol injection. The aberrant glucose metabolism was associated with a disorder in steroid biosynthesis induced by CI-AKI [30]. Although the precursor of anabolic steroids (cholesterol) was not directly detected, we observed a significant

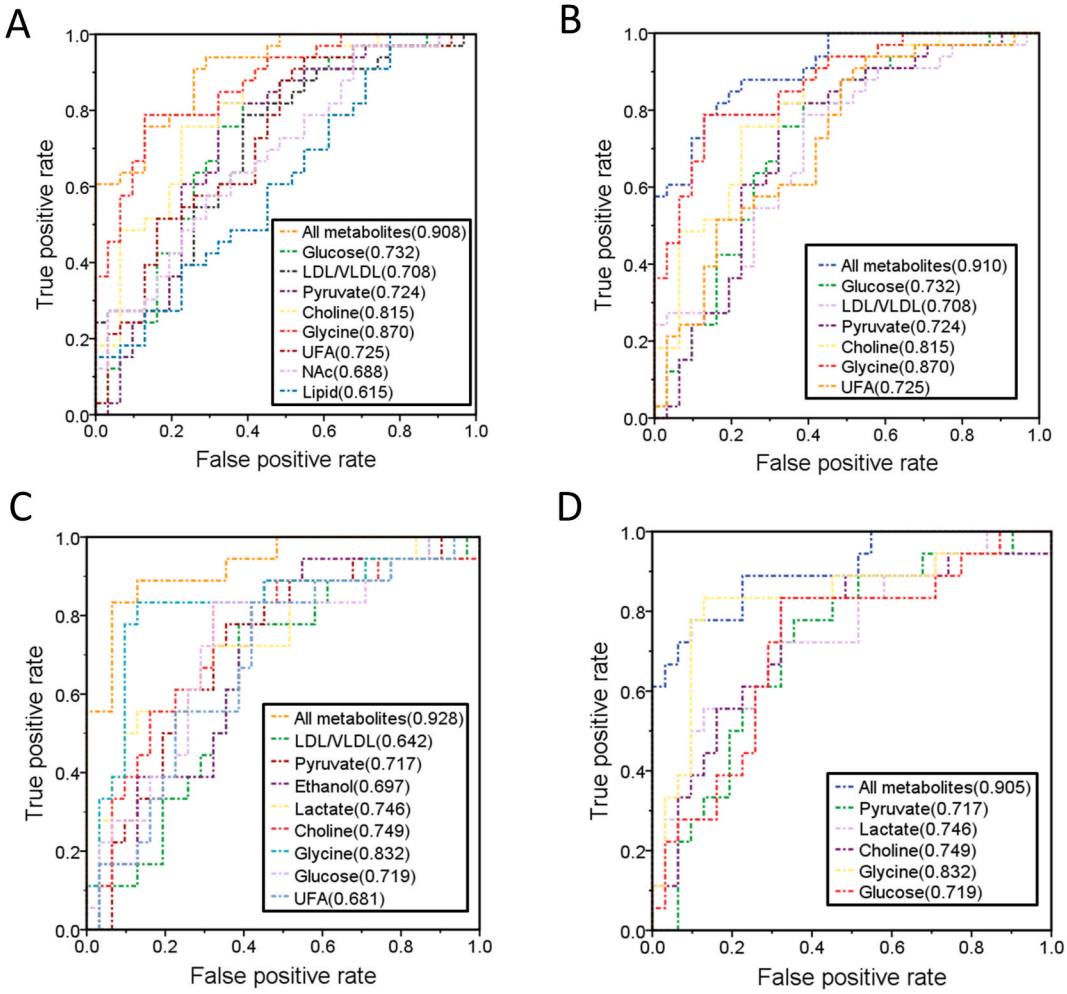

Fig. 7. Multivariate ROC curves assessing capabilities of the characteristic metabolites. (A) Multivariate ROC curves and AUC values of all characteristic metabolites at 24 h (post iodixanol injection) *vs.* 0 hr (prior to iodixanol administration); (B) Multivariate ROC curves of characteristic metabolites (AUC >0.70) at 24 h (post iodixanol injection) *vs.* 0 hr (prior to iodixanol administration); (C) Multivariate ROC curves and AUC values of all characteristic metabolites at 48 h (post iodixanol injection) *vs.* 0 hr (prior to iodixanol administration); (D) Multivariate ROC curves of characteristic metabolites (AUC >0.70) at 48 h (post iodixanol injection) *vs.* 0 hr (prior to iodixanol administration).

decrease in plasma NAc, the precursor of synthetic cholesterol, at 24 h post-iodixanol injection, suggesting that iodixanol might influence the metabolism of inorganic salts and sugars by reducing the biosynthesis of cholesterol or steroids.

The combined AUC value of the characteristic metabolites (AUC: 0.910 and 0.905 for the 24-h and 48-h groups, respectively) further underscored the dysregulation of glycolysis and amino acid metabolism following iodixanol injection. The activation of glycolysis and amino acid metabolism may impact the TCA cycle, which is intricately linked to energy metabolism. Given the high expression of AMP-activated protein kinase (AMPK) in kidney tissue, acute renal ischemia could swiftly activate the AMPK pathway, thereby influencing energy production and consumption pathways [31]. Previous studies have revealed that iohexol induced changes in over 30 metabolites (including pyruvate, choline, glycine, etc.) in the kidneys, plasma, and urine of CI-AKI rats, closely associated with disrupted energy and amino acid metabolism [20]. In CKD patients undergoing PCI, contrast media significantly induced mitochondrial dysfunction and oxidative stress in peripheral blood mononuclear cells (PBMCs) post-exposure, leading to decreased ATP levels and disturbed energy metabolism [32]. Our findings indicated a significant disturbance in the energy-related metabolic pathway following iodixanol injection, including glycine, serine, and threonine metabolism. Multivariate ROC curve analysis further validated the reliability of this pathway (AUC: 0.891 and 0.896). Additionally, we observed increased levels of glycine (a characteristic metabolite) in plasma, which could potentially serve as a biomarker, as indicated by the AUC values for the 24-h (0.870) and 48-h (0.832) groups. Furthermore, glycine serves as one of the precursors for glutathione synthesis. Glutathione plays a crucial role in scavenging excessive reactive oxygen species (ROS) and maintaining redox balance in vivo [33]. Therefore, we hypothesized that the elevated levels of glycine might be associated with oxidative stress induced by iodixanol.

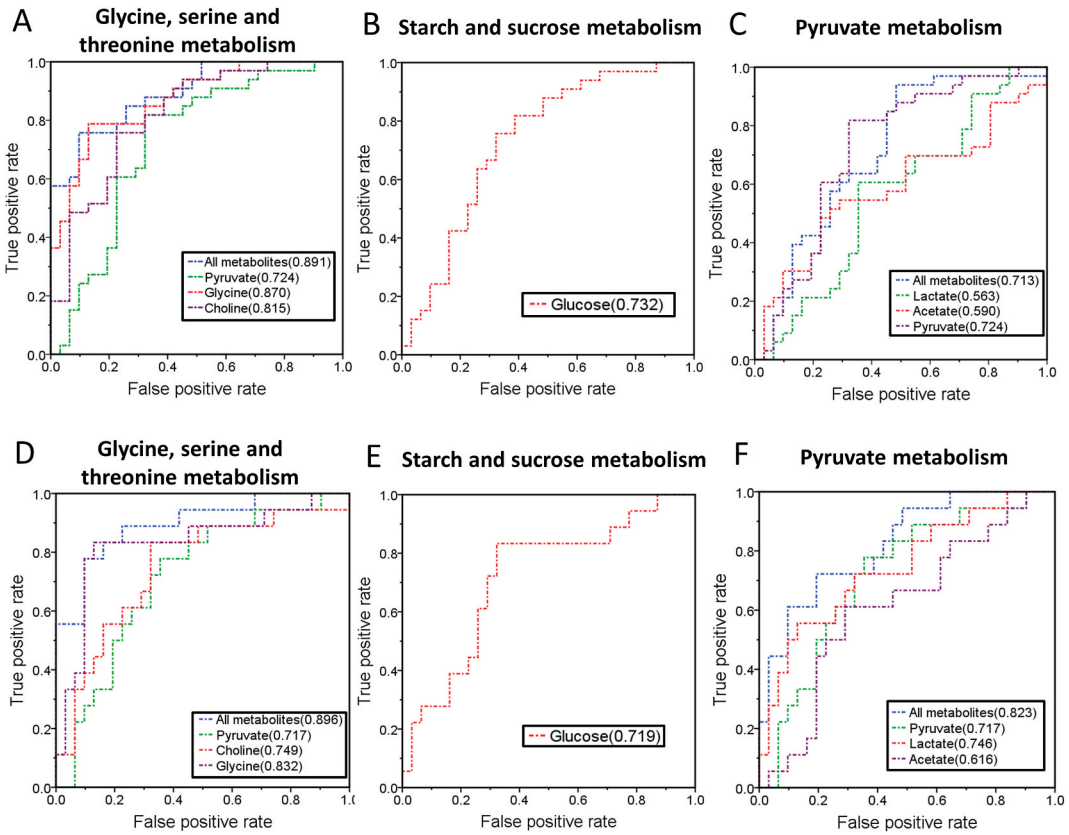

Fig. 8. Multivariate ROC curves assessing capabilities of the significantly disturbed metabolic pathways. The AUC values shown in brackets were used to evaluate the prediction performances of the biomarker models. (A, B, and C). Multivariate ROC curves of significantly disturbed metabolic pathways at 24 h (post iodixanol injection) *vs.* 0 hr (prior to iodixanol administration). (D, E, and F) Multivariate ROC curves of significantly disturbed metabolic pathways at 48 h (post iodixanol injection) *vs.* 0 hr (prior to iodixanol administration). (A, C) Glycine, serine, and threonine metabolism; (B, E) Starch and sucrose metabolism; (C, F) Pyruvate metabolism.

4.2. CM-increased fatty acid metabolism

It has been noted that the viscosity of CM could elevate blood viscosity, thereby impeding material exchange between various body tissues and organs, resulting in inadequate blood supply [34]. The enhancement of blood viscosity is associated with the content of UFA, which can ameliorate tissue microcirculation [35]. By modulating lipid levels in the blood, UFA can effectively enhance endothelial functions, mitigate vascular inflammation, and reduce blood pressure [36]. Our findings revealed a significant decrease in plasma UFA levels (a characteristic metabolite) at 24 and 48 h post-iodixanol injection. The diminished UFA levels may not be conducive to mitigating the increased blood viscosity caused by CM, potentially elevating the risk of adverse effects.

Additionally, AKI often accompanies lipid accumulation and dysregulation of energy metabolism in tubular epithelial cells [37]. Phosphorylation of acetyl-CoA carboxylase (ACC) by AMPK can inhibit fatty acid synthesis and promote fatty acid oxidation [31,37]. In this study, the decreased plasma UFA levels at 24 and 48 h post-iodixanol injection may indicate increased lipid accumulation and dysregulation of energy metabolism in tubular epithelial cells, exacerbating CM-induced kidney injury.

Furthermore, we observed a significant increase in plasma choline levels. Altered choline levels may affect fatty acid levels, thereby activating fatty acid catabolism [38]. The decreased levels of LDL/VLDL may be associated with vascular damage caused by iodixanol, where impaired blood vessels may compromise their ability to regulate LDL/VLDL metabolism, consequently reducing the transport capacity of endogenous cholesterol. Moreover, choline also participates in the metabolism of glycine, serine, and threonine, exhibiting high AUC values at the 24-h and 48-h groups (0.815 and 0.749). Therefore, choline might serve as a potential biomarker for early renal injury diagnosis.

5. Conclusion

CI-AKI represents an iatrogenic renal injury that has become increasingly prevalent among elderly patients due to the widespread use of CM. Hence, there is a pressing need to identify potential biomarkers for the early diagnosis of CI-AKI. Previously, our investigations revealed that iodixanol activated glucose metabolism while inhibiting choline and glutathione metabolism in endothelial

cells in vitro. In this current study, we examined the altered levels of metabolites in plasma samples obtained from elderly patients with CVD, which could potentially serve as early diagnostic biomarkers for iodixanol-induced renal injury. These identified metabolites are associated with glycolysis, fatty acid metabolism, and amino acid metabolism. This research contributes to the discovery of novel biomarkers and therapeutic targets for CI-AKI, thereby enhancing our understanding and management of this condition.

Ethical approval

This study was conducted in accordance with the Declaration of Helsinki. Ethical approval was granted by the Ethics Committee of Fujian Provincial Hospital (No. K2020-03-077, approval date: March 30, 2020).

Funding

This project was supported by Grant 32171174 and 31971357 from the National Natural Science Foundation of China; by Grant 2023A03J0531 from the Joint Funds from Guangzhou Science and Technology Project; by Grant ZDXK202103 from Guangzhou Key Discipline of Medicine (Geriatric Medicine, 2021–2023).

Data availability statement

The data used to support the findings of this study are available from https://www.ebi.ac.uk/metabolights/MTBLS9811.

CRediT authorship contribution statement

Qian Du: Writing – original draft, Project administration, Investigation. **Ting Jiang:** Writing – original draft, Software, Project administration, Methodology. **Qiuju Yuan:** Conceptualization, Data curation, Methodology. **Yuanyuan Bai:** Conceptualization, Data curation. **Donghai Lin:** Writing – review & editing, Supervision, Funding acquisition. **Donghui Liu:** Funding acquisition, Supervision, Writing – review & editing.

Declaration of competing interest

The authors declare the following financial interests/personal relationships which may be considered as potential competing interests: Donghui Liu and Donghai Lin reports financial support was provided by National Natural Science Foundation of China. Qian Du reports financial support was provided by the Joint Funds from Guangzhou Science and Technology Project. Donghui Liu reports financial support was provided by Guangzhou Key Discipline of Medicine (Geriatric Medicine, 2021–2023). If there are other authors, they declare that they have no known competing financial interests or personal relationships that could have appeared to influence the work reported in this paper.

Appendix A. Supplementary data

Supplementary data to this article can be found online at https://doi.org/10.1016/j.heliyon.2024.e30434.

References

[1] R. Mehran, G.D. Dangas, S.D. Weisbord, Contrast-associated acute kidney injury, N. Engl. J. Med. 380 (22) (2019) 2146–2155, https://doi.org/10.1056/NEJMra1805256.
[2] M. Almendarez, H.S. Gurm, J. Mariani Jr., M. Montorfano, E.S. Brilakis, R. Mehran, L. Azzalini, Procedural strategies to reduce the incidence of contrast-induced acute kidney injury during percutaneous coronary intervention, JACC Cardiovasc. Interv. 12 (19) (2019) 1877–1888, https://doi.org/10.1016/j.jcin.2019.04.055.
[3] E.A.J. Hoste, J.A. Kellum, N.M. Selby, A. Zarbock, P.M. Palevsky, S.M. Bagshaw, S.L. Goldstein, J. Cerda, L.S. Chawla, Global epidemiology and outcomes of acute kidney injury, Nat. Rev. Nephrol. 14 (10) (2018) 607–625, https://doi.org/10.1038/s41581-018-0052-0.
[4] P.A. McCullough, J.P. Choi, G.A. Feghali, J.M. Schussler, R.M. Stoler, R.C. Vallabahn, A. Mehta, Contrast-induced acute kidney injury, J. Am. Coll. Cardiol. 68 (13) (2016) 1465–1473, https://doi.org/10.1016/j.jacc.2016.05.099.
[5] P. Kusirisin, S.C. Chattipakorn, N. Chattipakorn, Contrast-induced nephropathy and oxidative stress: mechanistic insights for better interventional approaches, J. Transl. Med. 18 (1) (2020) 400, https://doi.org/10.1186/s12967-020-02574-8.
[6] A.L. Faucon, G. Bobrie, O. Clement, Nephrotoxicity of iodinated contrast media: from pathophysiology to prevention strategies, Eur. J. Radiol. 116 (2019) 231–241, https://doi.org/10.1016/j.ejrad.2019.03.008.
[7] A.S. Cheng, X. Li, The potential biotherapeutic targets of contrast-induced acute kidney injury, Int. J. Mol. Sci. 24 (9) (2023) 8254, https://doi.org/10.3390/ijms24098254.
[8] A. Narula, R. Mehran, G. Weisz, G.D. Dangas, J. Yu, P. Genereux, E. Nikolsky, S.J. Brener, B. Witzenbichler, G. Guagliumi, A.E. Clark, M. Fahy, K. Xu, B. R. Brodie, G.W. Stone, Contrast-induced acute kidney injury after primary percutaneous coronary intervention: results from the HORIZONS-AMI substudy, Eur. Heart J. 35 (23) (2014) 1533–1540, https://doi.org/10.1093/eurheartj/ehu063.
[9] C. Mamoulakis, K. Tsarouhas, I. Fragkiadoulaki, I. Heretis, M.F. Wilks, D.A. Spandidos, C. Tsitsimpikou, A. Tsatsakis, Contrast-induced nephropathy: basic concepts, pathophysiological implications and prevention strategies, Pharmacol. Ther. 180 (2017) 99–112, https://doi.org/10.1016/j.pharmthera.2017.06.009.

[10] M. Fahling, E. Seeliger, A. Patzak, P.B. Persson, Understanding and preventing contrast-induced acute kidney injury, Nat. Rev. Nephrol. Nephrology 13 (3) (2017) 169–180, https://doi.org/10.1038/nrneph.2016.196.
[11] C. Ronco, F. Stacul, P.A. McCullough, Subclinical acute kidney injury (AKI) due to iodine-based contrast media, Eur. Radiol. 23 (2) (2013) 319–323, https://doi.org/10.1007/s00330-012-2607-y.
[12] H.S. Thomsen, S.K. Morcos, R. Members of Contrast Media Safety Committee of European Society of Urogenital, In which patients should serum creatinine be measured before iodinated contrast medium administration? Eur. Radiol. 15 (4) (2005) 749–754, https://doi.org/10.1007/s00330-004-2591-y.
[13] M. Connolly, M. Kinnin, D. McEneaney, I. Menown, M. Kurth, J. Lamont, N. Morgan, M. Harbinson, Prediction of contrast induced acute kidney injury using novel biomarkers following contrast coronary angiography, QJM 111 (2) (2018) 103–110, https://doi.org/10.1093/qjmed/hcx201.
[14] C.R. Parikh, C. Liu, M.K. Mor, P.M. Palevsky, J.S. Kaufman, H. Thiessen Philbrook, S.D. Weisbord, Kidney biomarkers of injury and repair as predictors of contrast-associated AKI: a substudy of the preserve trial, Am. J. Kidney Dis. 75 (2) (2020) 187–194, https://doi.org/10.1053/j.ajkd.2019.06.011.
[15] M. Andreucci, T. Faga, E. Riccio, M. Sabbatini, A. Pisani, A. Michael, The potential use of biomarkers in predicting contrast-induced acute kidney injury, Int. J. Nephrol. Renovasc. Dis. 9 (2016) 205–221, https://doi.org/10.2147/IJNRD.S105124.
[16] C.B. Newgard, Metabolomics and metabolic diseases: where do we stand? Cell Metab. 25 (1) (2017) 43–56, https://doi.org/10.1016/j.cmet.2016.09.018.
[17] J.L. Markley, R. Bruschweiler, A.S. Edison, H.R. Eghbalnia, R. Powers, D. Raftery, D.S. Wishart, The future of NMR-based metabolomics, Curr. Opin. Biotechnol. 43 (2017) 34–40, https://doi.org/10.1016/j.copbio.2016.08.001.
[18] R.A. Silva, T.C.S. Pereira, A.R. Souza, P.R. Ribeiro, (1)H NMR-based metabolite profiling for biomarker identification, Clin. Chim. Acta 502 (2020) 269–279, https://doi.org/10.1016/j.cca.2019.11.015.
[19] S. Qiu, Y. Cai, H. Yao, C. Lin, Y. Xie, S. Tang, A. Zhang, Small molecule metabolites: discovery of biomarkers and therapeutic targets, Signal Transduct. Target. Ther. 8 (1) (2023) 132, https://doi.org/10.1038/s41392-023-01399-3.
[20] L. Wang, S. Huang, T. Zhu, X. Ge, C. Pei, G. Hong, L. Han, Metabolomic study on iohexol-induced nephrotoxicity in rats based on NMR and LC-MS analyses, Chem. Res. Toxicol. 35 (2) (2022) 244–253, https://doi.org/10.1021/acs.chemrestox.1c00299.
[21] D.B. Diercks, K.P. Owen, J.A. Kline, M.E. Sutter, Urine metabolomic analysis to detect metabolites associated with the development of contrast induced nephropathy, Clin. Exp. Emerg. Med. 3 (4) (2016) 204–212, https://doi.org/10.15441/ceem.15.110.
[22] N. Dalili, S. Chashmniam, S.M.H. Khoormizi, L. Salehi, S.A. Jamalian, M. Nafar, S. Kalantari, Urine and serum NMR-based metabolomics in pre-procedural prediction of contrast-induced nephropathy, Intern. Emerg. Med. 15 (1) (2020) 95–103, https://doi.org/10.1007/s11739-019-02128-x.
[23] L. Cheng, L. Wang, B. Chen, C. Wang, M. Wang, J. Li, X. Gao, Z. Zhang, L. Han, A multiple-metabolites model to predict preliminary renal injury induced by iodixanol based on UHPLC/Q-Orbitrap-MS and (1)H-NMR, Metabolomics 18 (11) (2022) 85, https://doi.org/10.1007/s11306-022-01942-3.
[24] T. Jiang, Q. Du, C. Huang, W. Xu, P. Guo, W. Li, X. Xie, Y. Guo, D. Liu, D. Lin, NMR-based metabolomic analysis on the protective effects of apolipoprotein A-I mimetic peptide against contrast media-induced endothelial dysfunction, Molecules 26 (17) (2021) 5123, https://doi.org/10.3390/molecules26175123.
[25] Y. Guo, W. Li, M. Qian, T. Jiang, P. Guo, Q. Du, N. Lin, X. Xie, Z. Wu, D. Lin, D. Liu, D-4F ameliorates contrast media-induced oxidative injuries in endothelial cells via the AMPK/PKC pathway, Front. Pharmacol. 11 (2021) 556074, https://doi.org/10.3389/fphar.2020.556074.
[26] J. Knuuti, W. Wijns, A. Saraste, D. Capodanno, E. Barbato, C. Funck-Brentano, E. Prescott, R.F. Storey, C. Deaton, T. Cuisset, S. Agewall, K. Dickstein, T. Edvardsen, J. Escaned, B.J. Gersh, P. Svitil, M. Gilard, D. Hasdai, R. Hatala, F. Mahfoud, J. Masip, C. Muneretto, M. Valgimigli, S. Achenbach, J.J. Bax, E.S.C. S.D. Group, ESC Guidelines for the diagnosis and management of chronic coronary syndromes, Eur. Heart J. 41 (3) (2019) 407–477, https://doi.org/10.1093/eurheartj/ehz425.
[27] P. Cui, C. Huang, J. Guo, Q. Wang, Z. Liu, H. Zhuo, D. Lin, Metabolic profiling of tumors, sera, and skeletal muscles from an orthotopic murine model of gastric cancer associated-cachexia, J. Proteome Res. 18 (4) (2019) 1880–1892, https://doi.org/10.1021/acs.jproteome.9b00088.
[28] S. Benito, A. Sanchez-Ortega, N. Unceta, F. Andrade, L. Aldamiz-Echevarria, M.A. Goicolea, R.J. Barrio, Untargeted metabolomics for plasma biomarker discovery for early chronic kidney disease diagnosis in pediatric patients using LC-QTOF-MS, Analyst 143 (18) (2018) 4448–4458, https://doi.org/10.1039/c8an00864g.
[29] M.T. James, S.M. Samuel, M.A. Manning, M. Tonelli, W.A. Ghali, P. Faris, M.L. Knudtson, N. Pannu, B.R. Hemmelgarn, Contrast-induced acute kidney injury and risk of adverse clinical outcomes after coronary angiography: a systematic review and meta-analysis, Circ. Cardiovasc. Interv. 6 (1) (2013) 37–43, https://doi.org/10.1161/CIRCINTERVENTIONS.112.974493.
[30] Y. Shu, C.L. Bello, L.M. Mangravite, B. Feng, K.M. Giacomini, Functional characteristics and steroid hormone-mediated regulation of an organic cation transporter in Madin-Darby canine kidney cells, J. Pharmacol. Exp. Ther. 299 (1) (2001) 392–398. https://jpet.aspetjournals.org/content/299/1/392.long.
[31] K.R. Hallows, P.F. Mount, N.M. Pastor-Soler, D.A. Power, Role of the energy sensor AMP-activated protein kinase in renal physiology and disease, Am. J. Physiol. Renal Physiol. 298 (5) (2010) F1067–F1077, https://doi.org/10.1152/ajprenal.00005.2010.
[32] P. Kusirisin, N. Apaijai, K. Noppakun, S. Kuanprasert, S.C. Chattipakorn, N. Chattipakorn, Circulating mitochondrial dysfunction as an early biomarker for contrast media-induced acute kidney injury in chronic kidney disease patients, J. Cell Mol. Med. 27 (14) (2023) 2059–2070, https://doi.org/10.1111/jcmm.17806.
[33] P. Vats, V.K. Singh, S.N. Singh, S.B. Singh, Glutathione metabolism under high-altitude stress and effect of antioxidant supplementation, Aviat. Space Envir. Med. 79 (12) (2008) 1106–1111, https://doi.org/10.3357/asem.2305.2008.
[34] E. Seeliger, M. Sendeski, C.S. Rihal, P.B. Persson, Contrast-induced kidney injury: mechanisms, risk factors, and prevention, Eur. Heart J. 33 (16) (2012) 2007–2015, https://doi.org/10.1093/eurheartj/ehr494.
[35] M.A.A. Rocha, A. van den Bruinhorst, W. Schroer, B. Rathke, M.C. Kroon, Physicochemical properties of fatty acid based ionic liquids, J. Chem. Thermodyn. 100 (2016) 156–164, https://doi.org/10.1016/j.jct.2016.04.021.
[36] C.E. Forsythe, S.D. Phinney, M.L. Fernandez, E.E. Quann, R.J. Wood, D.M. Bibus, W.J. Kraemer, R.D. Feinman, J.S. Volek, Comparison of low fat and low carbohydrate diets on circulating fatty acid composition and markers of inflammation, Lipids 43 (1) (2008) 65–77, https://doi.org/10.1007/s11745-007-3132-7.
[37] G. Harley, M. Katerelos, K. Gleich, D.P. de Souza, V.K. Narayana, B.E. Kemp, D.A. Power, P.F. Mount, Blocking AMPK signalling to acetyl-CoA carboxylase increases cisplatin-induced acute kidney injury and suppresses the benefit of metformin, Biomed. Pharmacother. 153 (2022) 113377, https://doi.org/10.1016/j.biopha.2022.113377.
[38] E. Currie, A. Schulze, R. Zechner, T.C. Walther, R.V. Farese, Cellular fatty acid metabolism and cancer, Cell Metab. 18 (2) (2013) 153–161, https://doi.org/10.1016/j.cmet.2013.05.017.